BIOCHEMISTRY
including biophysical chemistry & molecular biology

Article

pubs.acs.org/biochemistry

Transformations of the FeS Clusters of the Methylthiotransferases MiaB and RimO, Detected by Direct Electrochemistry

Stephanie J. Maiocco,[†] Arthur J. Arcinas,[‡] Bradley J. Landgraf,[§] Kyung-Hoon Lee,[§] Squire J. Booker,[‡,§,∥] and Sean J. Elliott*[,†]

[†]Department of Chemistry, Boston University, 590 Commonwealth Avenue, Boston, Massachusetts 02215, United States
[‡]Department of Biochemistry and Molecular Biology, [§]Department of Chemistry, and [∥]Howard Hughes Medical Institute, The Pennsylvania State University, University Park, Pennsylvania 16802, United States

Supporting Information

ABSTRACT: The methylthiotransferases (MTTases) represent a subfamily of the *S*-adenosylmethionine (AdoMet) radical superfamily of enzymes that catalyze the attachment of a methylthioether (-SCH_3) moiety on unactivated carbon centers. These enzymes contain two [4Fe-4S] clusters, one of which participates in the reductive fragmentation of AdoMet to generate a 5′-deoxyadenosyl 5′-radical and the other of which, termed the auxiliary cluster, is believed to play a central role in constructing the methylthio group and attaching it to the substrate. Because the redox properties of the bound cofactors within the AdoMet radical superfamily are so poorly understood, we have examined two MTTases in parallel, MiaB and RimO, using protein electrochemistry. We resolve the redox potentials of each [4Fe-4S] cluster, show that the auxiliary cluster has a potential higher than that of the AdoMet-binding cluster, and demonstrate that upon incubation of either enzyme with AdoMet, a unique low-potential state of the enzyme emerges. Our results are consistent with a mechanism whereby the auxiliary cluster is transiently methylated during substrate methylthiolation.

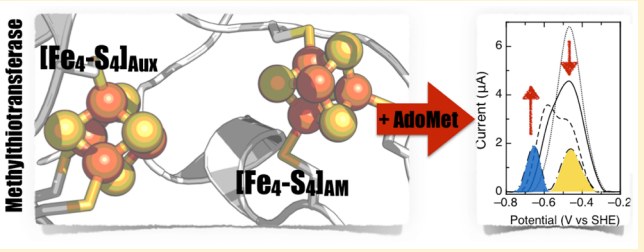

The *S*-adenosylmethionine (AdoMet) radical enzyme superfamily is composed of almost 114000 unique proteins catalyzing at least 65 distinct reactions, including the attachment of a methylthio (-SCH_3) group to unactivated carbon centers, catalyzed by members of the methylthiotransferase (MTTase) subfamily.[1−3] RimO[4−6] and MiaB[7,8] are two such MTTases, which install a methylthio group at C3 of Asp89 of ribosomal protein S12 and C2 of N^6-isopentenyladenosine (i^6A) in a number of tRNAs, respectively (Scheme 1). Despite the difference in their substrates, both RimO and MiaB are thought to catalyze their reactions by similar mechanisms. Both enzymes contain a canonical AdoMet radical [4Fe-4S] cluster (AM) that participates in the reductive cleavage of AdoMet to generate a 5′-deoxyadenosyl 5′-radical (5′-dA•), which then abstracts an appropriate hydrogen atom (H•) in the respective substrate. Both enzymes also bear an additional, or "auxiliary", [4Fe-4S] cluster, which has been postulated to be critical for MTTase chemistry.[6,8,9] However, the exact manner in which the auxiliary cluster participates in catalysis is currently unknown. The auxiliary clusters are ligated by three Cys residues, which leaves one iron ion with an available coordination site. The prevailing hypothesis is that this unique iron ion binds sulfide, which becomes methylated by AdoMet via a polar mechanism during the first step of catalysis. In the second step, initiated by H• abstraction by the 5′-dA•, the entire preformed methylthio group is transferred to its target via radical intermediates.[5,10,11]

Scheme 1

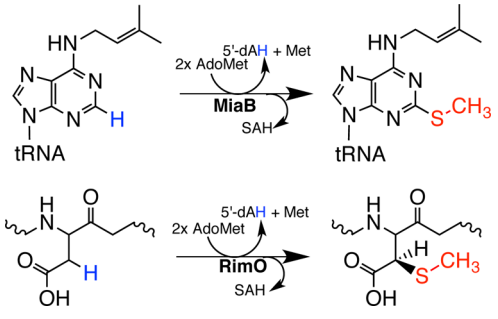

The auxiliary cluster has recently been shown to be accessible to bind Tris buffer,[12] and apo MiaB, when reconstituted with iron and selenide, catalyzes formation of 2-methylseleno-N^6-(isopentenyl)adenosine (mse^2i^6A) tRNA.[13] We hypothesize that investigating the redox properties of the unique auxiliary cluster of RimO and MiaB may lead to insight into the functional role it plays in MTTase chemistry. A structure available for the *Thermatoga maritima* (*Tm*) RimO (Figure 1) illustrates that the auxiliary cluster of the MTTase, where a

Received: July 1, 2016
Revised: August 11, 2016
Published: September 6, 2016

DOI: 10.1021/acs.biochem.6b00670
Biochemistry 2016, 55, 5531−5536

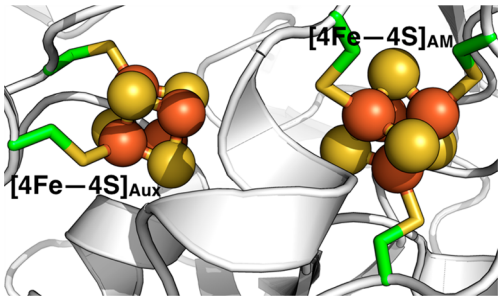

Figure 1. Structure of *Tm* RimO, revealing the two [4Fe-4S] clusters (Protein Data Bank entry 4jc0).

single iron site is available for binding with non-Cys ligands, is unlike the auxiliary clusters of AR dehydrogenases. In contrast, the auxiliary cluster of BtrN is bound entirely by four Cys ligands[14] and possesses a very low redox potential (−760 mV at pH 8).[15] Here, we have examined the redox potentials and reactivities of the FeS clusters of MiaB from *Bacteroides thetaiotaomicron* (*Bt*) and *Tm* RimO[7] using direct electrochemistry in order to gain a more detailed understanding of the MTTase subfamily of AR enzymes with a particular focus on elucidating the role of the auxiliary [4Fe-4S] cluster in the reaction. These efforts reveal that indeed, the MTTase auxiliary cluster has a potential much higher than that in BtrN, and that AdoMET-treatment yields a new enzyme form that may reflect the methylthiolated intermediate state.

EXPERIMENTAL PROCEDURES

Cloning and Expression of MiaB from *B. thetaiotaomicron*. *Bt* MiaB (NCBI accession number NP_812107.1) was amplified using polymerase chain reaction (PCR) technology from a pSGC-His construct obtained from Steven Almo (Albert Einstein University, Bronx, NY). The forward primer (5′-CGC GGC GTC CAT ATG AAC GAA TTA ACG GGA GCG GAC TTT AAA TCC-3′) contained a nine-nucleotide overhang sequence followed by an *Nde*I restriction site (underlined) and the first 33 bases of the *Bt miaB* gene. The reverse primer (5′-GAC TAA GCG CTC GAG CTA GAC TTC TTC GCC TTT CAG CGT AGC-3′) contained a nine-nucleotide overhang sequence, an *Xho*I restriction site (underlined), and the last 27 bases of the *Bt miaB* gene, including a stop codon. The PCR was performed on a Stratagene (Robocycler) Thermocycler. The product was isolated and digested with *Nde*I and *Xho*I and ligated into a pET28a vector (EMD Millipore, Billerica, MA) that had been similarly digested by standard procedures.[7] The correct construct, which contained a 10-amino acid linker between the N-terminal hexahistidine tag and the start codon of *Bt miaB*, was verified by DNA sequencing and termed pBtMiaB. *Tm* RimO was similarly amplified using PCR as previously described.[7] The pBtMiaB and pTmRimO expression constructs were transformed into *Ec* BL21(DE3) along with the pDB1282 construct containing the *isc* operon for Fe−S cluster assembly machinery from *Azotobacter vinelandii* as previously described.[16,17] The expression of *Bt miaB* and *Tm rimO* was performed similarly at 37 °C in 16 L of M9 minimal medium as previously described.[7]

Generation of the *Bt* MiaB AdoMet Cluster Triple Variant (C170, 174, 177A) and *Tm* RimO AdoMet Cluster Triple Variant (C150, 154, 157A). Mutagenesis was conducted using the Stratagene QuickChange II site-directed mutagenesis kit (Agilent, Santa Clara, CA) according to the manufacturer's specifications. The following primers were used to generate the *Bt* MiaB AdoMet cluster variant: the forward (5′-CC ATC ATG CGC GGA GCC AAT AAC TTC GCC ACC TAC GCT ATC GTG CCT TAT ACA CG-3′) and reverse (5′-CG TGT ATA AGG CAC GAT AGC GTA GGT GGC GAA GTT ATT GGC TCC GCG CAT GAT GG-3′) primers contained a 55-nucleotide sequence that is complementary to the *Bt miaB* gene with the underlined regions encoding the modified bases. The primers used to generate the *Tm* RimO AdoMet cluster variant were as follows: the forward (5′-CTG AAA ATT TCT GAA GGC GCT AAT CAC CGC GCC ACC TTC GCC ATT ATT CCG TCT ATG CGC-3′) and reverse (5′-GCG CAT AGA CGG AAT AAT GGC GAA GGT GGC GCG GTG ATT AGC GCC TTC AGA AAT TTT CAG-3′) primers contained a 60-nucleotide sequence that is complementary to the *Tm rimO* gene, with the underlined regions encoding the modified bases. Standard QuickChange II reaction mixtures contained the following in a 50 μL volume: 100 ng of pBtMiaB or pTmRimO, the forward and reverse primers each at 400 nM, each dNTP at 250 μM, 1× PFU Turbo DNA polymerase buffer, and 1 unit of PFU Turbo DNA polymerase. PCR conditions were as follows: 16 cycles of 95 °C for 1 min, 50 °C for 1.5 min, and 68 °C for 15 min, which was followed by incubation at 72 °C for 10 min and storage at 4 °C until use. The reaction mixture was then incubated with *Dpn*I enzyme (New England Biolabs, Ipswich, MA) at 37 °C overnight and then transformed into *Ec* DH5α. The correct sequences were confirmed by DNA sequencing and termed pBtMiaBTV or pTmRimOTV, accordingly. Expression of both gene constructs was conducted in *Ec* BL21(DE3) in the presence of pDB1282, as described above. *Tm* RimO was purified and chemically reconstituted as previously published.[7] The purification and chemical reconstitution of *Bt* MiaB was conducted like that of *Tm* MiaB, with the following exceptions. (1) The imidazole concentrations in the lysis and wash buffers were reduced to 10 and 20 mM, respectively. (2) The heat denaturation step was omitted. These procedures, in addition to the production of the 17-nucleotide RNA oligomer corresponding to the ACSL region of *Ec* $tRNA^{Phe}$, can be found elsewhere.[7]

Nonturnover Protein Film Electrochemistry. Electrochemical experiments were performed anaerobically in an MBraun Labmaster glovebox using a PGSTAT 12 potentiostat (EcoChemie). A three-electrode configuration was used in a water-jacketed glass cell. A platinum wire was used as the counter electrode, and the reference electrode was a standard calomel electrode; potentials reported are relative to the standard hydrogen electrode.

Baseline measurements were collected using a pyrolytic graphite edge (PGE) electrode polished with 1 μm alumina, rinsed, and placed in a glass cell containing a 10 °C mixed buffer solution (10 mM MES, CHES, TAPS, and HEPES) (pH 8.0) with 200 mM NaCl. A 3 μL aliquot of 2.24 mM protein was applied directly to the polished PGE electrode surface along with 15 mg/mL polymyxin B sulfate (Sigma). The protein sample was removed after 5 min, and the electrode was placed back into the buffer cell solution. Nonturnover electrochemical signals were analyzed by correction of the non-Faradaic component of the current from the raw data using the SOAS package (as described in ref 15).

Examination of AdoMet Binding via Protein Film Voltammetry. Examination of AdoMet binding was performed in square wave voltammetry mode with a potential

DOI: 10.1021/acs.biochem.6b00670
Biochemistry 2016, 55, 5531−5536

window of −1.0 to 0 V (vs SHE) using the same buffer system described above (pH 8.0) at a total cell volume of 500 μL and confirmed with cyclic voltammetry. The following square wave voltammetry parameters were used: a frequency of 10 Hz with an amplitude of 20 mV or a frequency of 200 Hz with an amplitude of 50 mV. Measurements were first taken in the absence of AdoMet, and after AdoMet had been added to a final concentration of 400 μM, measurements were taken again.

Electrochemistry with *S*-Adenosylhomocysteine and Methanethiol. Examination of *S*-adenosylhomocysteine (AdoHCys) and methanethiol binding was performed in square wave mode using the same buffer used above (pH 8.0). Measurements were taken in the absence of AdoHcys and/or methanethiol, and then the omitted components were added to achieve a total cell volume of 500 μL and final concentrations ranging from 200 μM to 7 mM. Scans were taken immediately and every 5−10 min for a total of 40 min, or until no additional changes were observed.

Binding of Substrate via Protein Film Electrochemistry. Examination of tRNA binding was performed in square wave mode using the same buffer described above (pH 8.0). Measurements were taken in the absence of tRNA, and then tRNA was added to achieve a total cell volume of 500 μL and final concentrations ranging from 10 to 130 μM. Scans were taken immediately and every 5−10 min for a total of 40 min, or until no additional changes were observed.

Electrochemistry with AdoMet Reductive Cleavage Products. The impact of the reductive cleavage products, 5′-deoxyadenosine (5′-dAH) and methionine, was examined in square wave mode using the same buffer that was used above (pH 8.0). Measurements were taken in the absence of products, and then 5′-deoxyadenosine, methionine, and substrate tRNA were added to the cell solution to achieve a total cell volume of 500 μL and final concentrations ranging from 500 μM to 1.3 mM.

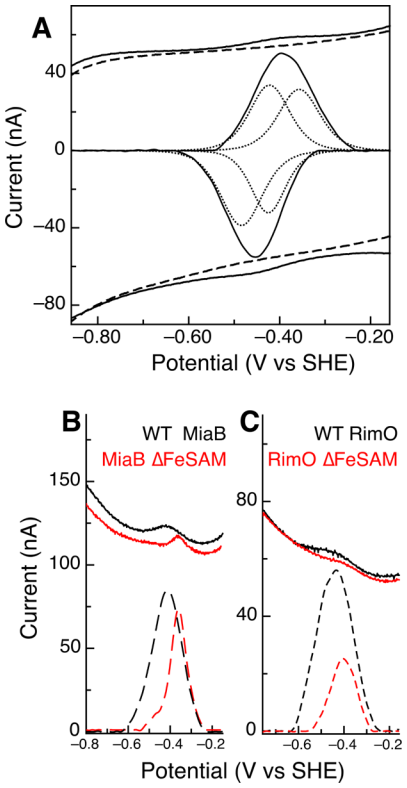

Figure 2. Voltammetry of *Bt* MiaB and *Tm* RimO. (A) Cyclic voltammetry of *Bt* MiaB, with a scan rate of 100 mV/s, at pH 8.0 and 10 °C. (B) Square wave voltammetry of wild-type *Bt* MiaB (black) and ΔFeS_{AM} protein (red), collected with a frequency of 10 Hz and an amplitude of 20 mV. (C) Square wave data of wild-type *Tm* RimO (black) and ΔFeS_{AM} protein (red). Dashed lines in panels B and C indicate the data corrected for the background response of the electrode.

RESULTS

Similar to our efforts with BtrN, we used protein film electrochemistry (PFE) as a tool to examine the redox characteristics of the two [4Fe-4S] clusters of *Bt* MiaB and *Tm* RimO. As in our studies of BtrN[15] and TsrM,[18] graphite electrodes were successfully employed to generate voltammetric data for the enzymes, and polymixin was found to be a required co-adsorbate. As with BtrN, square wave voltammetry (SWV) was used in parallel with cyclic voltammetry (CV) experiments to maximize the sensitivity of the analysis. For example, CV data for *Bt* MiaB (Figure 2A) revealed a single, quasi-reversible feature with a non-zero peak separation and an average peak width at half-height of 140 mV, nearly twice that of the predicted value of 86 mV, which would indicate a simple one-electron feature.[19] While the peak separation is taken to indicate slow electron transfer rates, the data could be readily fit to two one-electron redox couples with potentials of −450 and −390 mV. The CV data were further confirmed with SWV (Figure 2B). On the basis of previous reports of MiaB indicating that the protein is purified with the auxiliary cluster partially reduced, the couple at −390 mV was presumed to be the $[4Fe\text{-}4S]^{2+/+}_{Aux}$ couple. To confirm this hypothesis, the triple variant containing only the auxiliary cluster and missing the AdoMet-binding cluster (ΔFeS_{AM}) was examined (Figure 2B). A single feature at approximately −400 mV was observed for *Bt* MiaB ΔFeS_{AM}, with a significantly narrowed peak width at half-height (93 mV), fitting within the envelope of the wild-type enzyme. Thus, we concluded that with respect to the fitting of the CV data, the lower-potential −450 mV feature likely corresponds to the $[4Fe\text{-}4S]^{2+/+}_{AM}$ couple, and the higher feature at −390 mV is due to the $[4Fe\text{-}4S]^{2+/+}_{Aux}$ cluster in MiaB.

Tm RimO proved to be similar, though not identical: electroactive film coverages for *Tm* RimO were lower than those of *Bt* MiaB, preventing the assignment of two potentials via CV (yet it was clear that the overall voltammogram was shifted more negative when compared to that of *Bt* MiaB by 40 mV). However, by SWV methods, we could compare the two MTTases and distinguish the wild-type and ΔFeS_{AM} *Tm* enzymes (Figure 2C). As with *Bt* MiaB, wild-type *Tm* RimO showed a broad SWV signal (−420 mV) that narrowed in comparison with that of the ΔFeS_{AM} construct, appearing at a more positive potential (−405 mV). Thus, we find that the *Tm* RimO [4Fe-4S] redox potentials appear to be highly similar to those of *Bt* MiaB: the auxiliary cluster is more positive than the AdoMet-binding cluster by roughly 60 mV, though overall, RimO resting state redox potentials (with no added ligand) appear to be shifted to more negative potentials compared to those of MiaB by approximately 40 mV.

MTTases exploit the reactivity of the $[4Fe\text{-}4S]_{AM}$ cluster with AdoMet to produce 5′-dA• and also use AdoMet as a source of a methyl moiety.[7] Thus, we examined the reactivity of MiaB and RimO with AdoMet, recognizing that previous studies of AR enzymes lysine 2,3-aminomutase[20] and BtrN[15] have

DOI: 10.1021/acs.biochem.6b00670
Biochemistry 2016, 55, 5531−5536

indicated that upon binding AdoMet, the potential of the AdoMet-binding cluster shifts to more positive values. For both MiaB and RimO, AdoMet was added to the cell solution following the generation of the protein film. To ensure accurate comparisons between the enzymes and to heighten sensitivity, SWV was used as the sole PFE detection modality, and a saturating concentration of AdoMet was used. Figure 3A shows

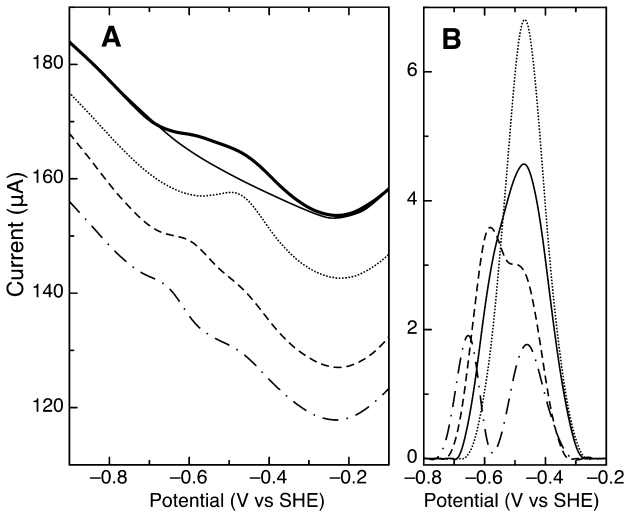

Figure 3. (A) SWV of *Bt* MiaB (heavy solid line) compared to bare graphite electrodes (light solid line) and with addition of 1.6 mM AdoMet (···) and further incubation *in situ* for 10 min (---) and 20 min (·—·). (B) Data from panel A, but corrected for the non-Faradaic component of the current. All data were recorded with a frequency of 200 Hz and an E_{amp} of 50 mV at pH 8 and 10 °C.

the raw data, indicating time-dependent changes in the results of *Bt* MiaB voltammetry upon addition of AdoMet to the adsorbed enzyme. Background-subtracted data are given in Figure 3B. Immediately upon AdoMet addition (within 10−15 s), the electrochemical feature becomes sharper with an overall shift to a more positive potential (increasing by 60 mV). Upon further incubation over 10 min, two distinct features emerge, one of which is at −415 mV with a peak width at half-height of 110 mV, consistent with a one-electron center. After incubation for 20 min, the lower-potential feature is observed at −615 mV (Figure 3A). After that point, no further transformation can be observed.

In the comparison, *Tm* RimO revealed similar though not identical behavior in the presence of AdoMet: there is an initial shift of the electrochemical envelope of +50 mV, and a resulting second, low-potential feature, which in the case of RimO has a final observed potential of −580 mV (Figure 4). As with MiaB, the electrochemically detected changes in RimO are complete in 20 min, and in both cases, the final stoichiometries of the two states generated (estimated by their electrochemical areas) are essentially 1:1, indicating a complete transformation of the resting enzyme. In both cases, neither further addition of AdoMet nor monitoring on longer time scales resulted in either the recovery of the initial resting state signal or any further changes. However, in contrast to what is observed in MiaB, the lowest-potential state formed by RimO does not develop over 20 min and instead is generated as quickly as mixing can occur in the electrochemical cell (Figure 4B, dotted line), yet we believe that the overall model of reactivity is the same. First, an event occurs that we interpret as ligand binding, which results

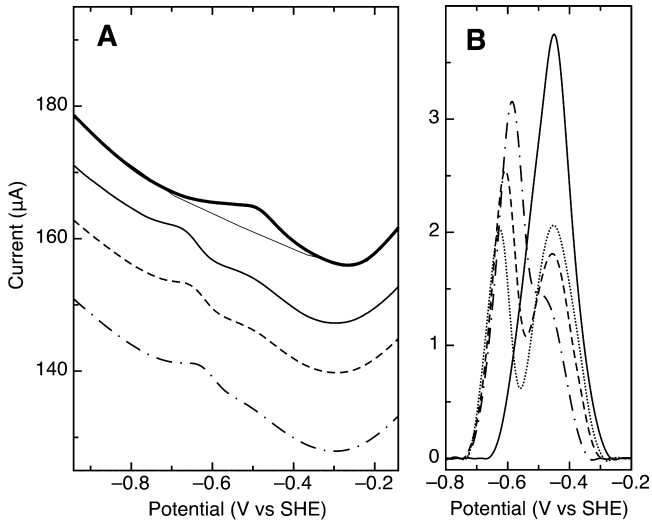

Figure 4. (A) Equivalent SWV data for *Tm* RimO (thick solid line) compared to a bare graphite electrode (light solid line) and with addition of 1.6 mM AdoMet (···) and further incubation for 10 min (---) and 20 min (·—·). (B) Data from panel panel A, but corrected for the non-Faradaic component of the current. All data were collected with a frequency of 200 Hz and an E_{amp} of 50 mV at pH 8 and 10 °C.

in a positive shift in potential as observed in MiaB, but is absent in the RimO data; then a subsequent step produces a new species of very low (less than −600 mV) potential. In the case of RimO, the lowest-potential species generated immediately represents a precursor that transforms on a time scale similar to that of MiaB, arriving at the final state marked by a potential of approximately −600 mV. A tantalizing possibility is that this final low-potential state may represent a methylated version of each MTTase at the auxiliary cluster, arising from the reaction with AdoMet. Consistent with this possibility, previous studies have shown that when *Tm* RimO or *Tm* MiaB is incubated with AdoMet in the absence of a low-potential reductant, methanethiol can be liberated from either protein upon acid treatment.[7]

To further assess the nature of the low-potential states resulting from AdoMet treatment, we examined the reactions of MiaB and RimO with readily available products of their reactions: AdoHCys, 5′-dAH, and Met. Of these, only AdoHCys noticeably affected MiaB and RimO redox characteristics. In each case, binding of AdoHcys shifts the observed voltammetric feature in the positive direction by 40 mV (Figure S1) and gives rise to an increased intensity, indicative of faster electrokinetics. Such a shift has been noted for the $[4Fe\text{-}4S]_{AM}$ cluster of BtrN, and we believe here the same impact is felt at the AdoMet-binding active site. To mimic the impact of internal methyl transfer, RimO and MiaB were also examined electrochemically in the presence of sodium methanethiolate (Figure S2), which has been shown to act as a surrogate methylthio donor with *Tm* RimO and MiaB. Treatment with the methanethiolate modestly shifted the overall SWV envelope to a more negative potential, but only by −30 mV in the case of RimO and −80 mV in the case of MiaB. In neither case could methanethiolate recapitulate the impact of AdoMet, where a low-potential state was achieved over time.

Finally, we examined the potential impact of an MTTase substrate upon the electrochemical response of MiaB. Analogous SWV experiments were performed with MiaB adsorbed at a graphite electrode and using a 17-base tRNA

DOI: 10.1021/acs.biochem.6b00670
Biochemistry 2016, 55, 5531−5536

oligonucleotide corresponding to the anticodon stem loop of wild-type $tRNA^{Phe}$ as a substrate.[7,13] In the presence of a maximal concentration of 130 μM i^6A tRNA, minimal shifts [less than −30 mV (Figure S3)] were observed. Further, addition of tRNA to MiaB previously treated with AdoMet did not yield an observable electrochemical response, suggesting that if the enzyme has undergone the first steps of reactivity with AdoMet, subsequent substrate binding desorbs the enzyme from the electrode or creates a conformation that prevents fast electrochemical communication.

DISCUSSION

Collectively, we have now shed further light on the redox chemistry of the AR MTTase subfamily using direct electrochemical methods to assess the FeS clusters of both *Tm* RimO and *Bt* MiaB. We have demonstrated that the $[4Fe\text{-}4S]^{2+/+}_{AM}$ redox potentials for the MTTase are in good agreement with those reported previously for other AR enzyme active site clusters. However, our data show a distinct contrast between the potentials for "auxiliary" clusters: those of the MTTase subfamily reported here for both MiaB and RimO are significantly higher than the −760 mV value for BtrN,[15] the only $[4Fe\text{-}4S]_{Aux}$ cluster redox potential that has been reported. This difference may be associated with the function of the auxiliary clusters in these two enzyme subfamilies.

We have demonstrated not only that RimO and MiaB are electrochemically active, but also that their electrochemistry reveals reactivity with AdoMet in an unprecedented way, when compared to the electrochemical traits of other AR enzymes. In both cases, we find that on an electrochemically detectable time scale, MiaB and RimO both yield a low-potential state in the presence of AdoMet, which cannot be attributed to the binding of product. A hypothetical model (Scheme 2) shows how the

Scheme 2

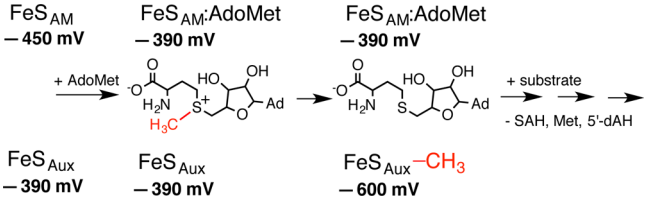

resting state of either enzyme is marked by potentials that are close to each other and that AdoMet binds to either MTTase in a fashion that makes both potentials nearly identical. Methyl transfer follows from one of the two required AdoMet molecules bound at an unknown location, which is suggested to modify the $[4Fe\text{-}4S]_{Aux}$ cluster, leading to a version of the cluster with a very low redox potential (approximately −600 mV). Following substrate binding and 5′-dA$^\bullet$ generation at the $[4Fe\text{-}4S]_{AM}$ cluster, abstraction of H$^\bullet$ from the substrate proceeds and thiomethyl transfer is effected. However, we note that the data presented here cannot distinguish the ordering of steps in the possible reaction directly. In other words, our data cannot determine whether two AdoMet molecules bind to both RimO and MiaB or if a single AdoMet molecule binds and reacts with what we believe to be the $[4Fe\text{-}4S]_{Aux}$ cluster, prior to the binding of either substrate and/or a second molecule of AdoMet. However, AdoMet-binding sites in addition to the canonical $[4Fe\text{-}4S]_{AM}$ cluster are not apparent in the RimO crystal structure.

In addition, we have noted that *Tm* RimO's AdoMet-dependent chemistry is even more complex: a "lowest-potential" state is generated as quickly as hand mixing allows for a measurement (10−20 s), faster than the time scale associated with steady state catalysis,[7] and therefore precluding assignment of that initial species to a methylated product. Following its initial inception, the value of the lowest-potential species increases slightly (to −580 mV in RimO), consistent with a decay of the initial product and with the time scale associated with methylation. Thus, we believe that in the case of both MTTases, we arrive at the same final product, though through distinct kinetic steps. One possibility for these apparent kinetic differences between *Bt* MiaB and *Tm* RimO is that the first electrochemically detected product formed by each enzyme differs in terms of the fates of the SAH byproduct, or conformational rearrangements of the relatively plastic active sites.

Our data also evoke questions regarding the functional significance of the low-potential states observed here. It is possible there is a functional advantage of having a low-potential methylated FeS cluster: the low potential is likely advantageous for intercepting a radical species generated at the $[4Fe\text{-}4S]_{AM}$ active site; also, if the potential of the methylated state were significantly higher, that species may provide a thermodynamic sink for reduction via $[4Fe\text{-}4S]_{AM}$, potentially preventing catalysis. With these rationales in hand, we are in the position of being able to examine the impact of the auxiliary cluster environment upon the redox potential of the auxiliary cluster itself, the resultant impact upon reactivity with AdoMet, and to further characterize the redox characteristics of transitory redox states generated therein. Finally, we note that it is challenging to compare the low-potential electrochemical signals observed here with precedents from the synthetic literature, as we do not know of a specific model system that directly mimics the properties of either MiaB or RimO. While Holm and colleagues have produced site-differentiated [4Fe-4S] clusters,[21,22] making use of a chelating 1,3,5-tris[(4,6-dimethyl-3-mercaptophenyl)thio]-2,4,6-tris(*p*-tolylthio)-benzenate ligand that leaves one iron exposed to bind additional ligands, direct comparison with a sulfido- and methylthiolate-bound cluster is not easy. While various alkyl- and arylthiolate versions have been reported, including their redox potentials, the sulfido-bound compound was found to dimerize into a sulfido-bridged set of clusters,[22] clearly not identical to either MiaB or RimO.

With respect to the potential open coordination site in the auxiliary cluster of both MiaB and the crystallographically characterized RimO (Figure 1), there have been proposals that an open site on the auxiliary cluster serves to bind substrate (in addition to, or instead of, a methyl moiety).[11] To investigate this hypothesis, we monitored the impact of tRNA binding, finding that redox potentials of the FeS clusters shift by less than 30 mV, suggesting that tRNA does not bind to the auxiliary cluster directly. In particular, these small changes in potential could be attributed to overall charging effects of adding a polyionic species. Our efforts using direct electrochemistry illustrate the challenges associated with studying such complex enzymes that modify large substrates. In our efforts reported here, we have used only graphite electrodes that are capable of visiting the low potentials associated with the FeS clusters themselves. Addition of tRNA to films of MiaB that have already been exposed to AdoMet did not yield any discernible electrochemical data, suggesting that binding of an

DOI: 10.1021/acs.biochem.6b00670
Biochemistry 2016, 55, 5531−5536

RNA to the AdoMet-treated enzyme results in a conformation that does not allow for direct electrochemical communication. In the future, tRNA binding could be further assessed by using tRNA-modified electrodes.[23] However, our results are also mimicked by no obvious changes in the resonance Raman or EPR spectra of MiaB in the presence of tRNA.[10]

■ ASSOCIATED CONTENT

Supporting Information

The Supporting Information is available free of charge on the ACS Publications website at DOI: 10.1021/acs.biochem.6b00670.

Supporting electrochemistry control experiments (PDF)

■ AUTHOR INFORMATION

Corresponding Author

*Boston University, 590 Commonwealth Ave., Boston, MA 02215. Telephone: 617-358-2816. E-mail: elliott@bu.edu.

Funding

This work has been supported by the National Institutes of Health [GM-101957 (S.J.B. and S.J.E.) and GM-120283 (S.J.E.)] and the Howard Hughes Medical Institute (S.J.B.).

Notes

The authors declare no competing financial interest.

■ ABBREVIATIONS

5′-dA, 5′-deoxyadenosine; 5′-dA•, 5′-deoxyadenosyl 5′-radical; AdoHCys, *S*-adenosylhomocysteine; AdoMet, *S*-adenosylmethionine; AR, AdoMet radical; *Bt*, *B. thetaiotaomicron*; CV, cyclic voltammetry; *Ec*, *Escherichia coli*; FeS, iron sulfur; Met, methionine; MTTase, methylthiotransferase; PFE, protein film electrochemistry; *Tm*, *T. maritima*; SWV, square wave voltammetry.

■ REFERENCES

(1) Bauerle, M. R., Schwalm, E. L., and Booker, S. J. (2015) Mechanistic diversity of radical *S*-adenosylmethionine (SAM)-dependent methylation. *J. Biol. Chem. 290*, 3995−4002.

(2) Dowling, D. P., Vey, J. L., Croft, A. K., and Drennan, C. L. (2012) Structural diversity in the adomet radical enzyme superfamily. *Biochim. Biophys. Acta, Proteins Proteomics 1824*, 1178−1195.

(3) Akiva, E., Brown, S., Almonacid, D. E., Barber, A. E., 2nd, Custer, A. F., Hicks, M. A., Huang, C. C., Lauck, F., Mashiyama, S. T., Meng, E. C., Mischel, D., Morris, J. H., Ojha, S., Schnoes, A. M., Stryke, D., Yunes, J. M., Ferrin, T. E., Holliday, G. L., and Babbitt, P. C. (2014) The structure-function linkage database. *Nucleic Acids Res. 42*, D521−530.

(4) Anton, B. P., Saleh, L., Benner, J. S., Raleigh, E. A., Kasif, S., and Roberts, R. J. (2008) RimO, a MiaB-like enzyme, methylthiolates the universally conserved Asp88 residue of ribosomal protein S12 in *Escherichia coli*. *Proc. Natl. Acad. Sci. U. S. A. 105*, 1826−1831.

(5) Lee, K. H., Saleh, L., Anton, B. P., Madinger, C. L., Benner, J. S., Iwig, D. F., Roberts, R. J., Krebs, C., and Booker, S. J. (2009) Characterization of rimo, a new member of the methylthiotransferase subclass of the radical SAM superfamily. *Biochemistry 48*, 10162−10174.

(6) Arragain, S., Garcia-Serres, R., Blondin, G., Douki, T., Clemancey, M., Latour, J. M., Forouhar, F., Neely, H., Montelione, G. T., Hunt, J. F., Mulliez, E., Fontecave, M., and Atta, M. (2010) Post-translational modification of ribosomal proteins: Structural and functional characterization of RimO from *Thermotoga maritima*, a radical *S*-adenosylmethionine methylthiotransferase. *J. Biol. Chem. 285*, 5792−5801.

(7) Landgraf, B. J., Arcinas, A. J., Lee, K. H., and Booker, S. J. (2013) Identification of an intermediate methyl carrier in the radical *S*-adenosylmethionine methylthiotransferases RimO and MiaB. *J. Am. Chem. Soc. 135*, 15404−15416.

(8) Forouhar, F., Arragain, S., Atta, M., Gambarelli, S., Mouesca, J. M., Hussain, M., Xiao, R., Kieffer-Jaquinod, S., Seetharaman, J., Acton, T. B., Montelione, G. T., Mulliez, E., Hunt, J. F., and Fontecave, M. (2013) Two Fe-S clusters catalyze sulfur insertion by radical-SAM methylthiotransferases. *Nat. Chem. Biol. 9*, 333−338.

(9) Booker, S. J., Cicchillo, R. M., and Grove, T. L. (2007) Self-sacrifice in radical *S*-adenosylmethionine proteins. *Curr. Opin. Chem. Biol. 11*, 543−552.

(10) Hernandez, H. L., Pierrel, F., Elleingand, E., Garcia-Serres, R., Huynh, B. H., Johnson, M. K., Fontecave, M., and Atta, M. (2007) MiaB, a bifunctional radical-*S*-adenosylmethionine enzyme involved in the thiolation and methylation of tRNA, contains two essential [4Fe-4S] clusters. *Biochemistry 46*, 5140−5147.

(11) Jarrett, J. T. (2015) The biosynthesis of thiol- and thioether-containing cofactors and secondary metabolites catalyzed by radical *S*-adenosylmethionine enzymes. *J. Biol. Chem. 290*, 3972−3979.

(12) Molle, T., Clemancey, M., Latour, J. M., Kathirvelu, V., Sicoli, G., Forouhar, F., Mulliez, E., Gambarelli, S., and Atta, M. (2016) Unanticipated coordination of tris buffer to the radical SAM cluster of the RimO methylthiotransferase. *JBIC, J. Biol. Inorg. Chem. 21*, 549−557.

(13) Pierrel, F., Douki, T., Fontecave, M., and Atta, M. (2004) Miab protein is a bifunctional radical-*S*-adenosylmethionine enzyme involved in thiolation and methylation of tRNA. *J. Biol. Chem. 279*, 47555−47563.

(14) Goldman, P. J., Grove, T. L., Booker, S. J., and Drennan, C. L. (2013) X-ray analysis of butirosin biosynthetic enzyme BtrN redefines structural motifs for AdoMet radical chemistry. *Proc. Natl. Acad. Sci. U. S. A. 110*, 15949−15954.

(15) Maiocco, S. J., Grove, T. L., Booker, S. J., and Elliott, S. J. (2015) Electrochemical resolution of the [4Fe-4S] centers of the adomet radical enzyme BtrN: Evidence of proton coupling and an unusual, low-potential auxiliary cluster. *J. Am. Chem. Soc. 137*, 8664−8667.

(16) Cicchillo, R. M., Lee, K. H., Baleanu-Gogonea, C., Nesbitt, N. M., Krebs, C., and Booker, S. J. (2004) Escherichia coli lipoyl synthase binds two distinct [4Fe-4S] clusters per polypeptide. *Biochemistry 43*, 11770−11781.

(17) Lanz, N. D., Grove, T. L., Gogonea, C. B., Lee, K. H., Krebs, C., and Booker, S. J. (2012) RlmN and AtsB as models for the overproduction and characterization of radical SAM proteins. *Methods Enzymol. 516*, 125−152.

(18) Blaszczyk, A. J., Silakov, A., Zhang, B., Maiocco, S. J., Lanz, N. D., Kelly, W. L., Elliott, S. J., Krebs, C., and Booker, S. J. (2016) Spectroscopic and electrochemical characterization of the iron-sulfur and cobalamin cofactors of TsrM, an unusual radical *S*-adenosylmethionine methylase. *J. Am. Chem. Soc. 138*, 3416−3426.

(19) Léger, C., and Bertrand, P. (2008) Direct electrochemistry of redox enzymes as a tool for mechanistic studies. *Chem. Rev. 108*, 2379−2438.

(20) Hinckley, G. T., and Frey, P. A. (2006) Cofactor dependence of reduction potentials for [4Fe-4S] 2+/1+ in lysine 2, 3-aminomutase. *Biochemistry 45*, 3219−3225.

(21) Venkateswara Rao, P., and Holm, R. H. (2004) Synthetic analogues of the active sites of iron-sulfur proteins. *Chem. Rev. 104*, 527−560.

(22) Zhou, C. Y., and Holm, R. H. (1997) Comparative isotropic shifts, redox potentials, and ligand binding propensities of [1:3] site-differentiated cubane-type $[Fe_4q_4]^{2+}$ clusters (q = S, Se). *Inorg. Chem. 36*, 4066−4077.

(23) Wang, J., Kawde, A. N., and Sahlin, E. (2000) Renewable pencil electrodes for highly sensitive stripping potentiometric measurements of DNA and RNA. *Analyst 125*, 5−7.

DOI: 10.1021/acs.biochem.6b00670
Biochemistry 2016, 55, 5531−5536